SETTING UP THE PRESERVATION OF FLUVIAL CHANNEL BELTS

Benjamin T. Cardenas[1,2]*, John M. Swartz[1,3,4,5], David Mohrig[1], and Eric W. Prokocki[1]

[1]Jackson School of Geosciences, The University of Texas at Austin, Austin, TX, USA

[2]now at Division of Geological and Planetary Sciences, California Institute of Technology, Pasadena, CA, USA

[3]Institute for Geophysics, Jackson School of Geosciences, The University of Texas at Austin, Austin, TX, USA

[4]Department of Civil, Architectural, and Environmental Engineering, The University of Texas at Austin, Austin, TX, USA

[5]Department of Geosciences, Boise State University, Boise, ID, USA

*Corresponding author email: bencard@caltech.edu

THIS MANUSCRIPT HAS NOT COMPLETED THE PEER-REVIEW PROCESS

ABSTRACT

Subsidence alone is often too slow to create the necessary relief needed to preserve continuous channel belts over 10s of km, as are often observed in outcrops on Earth and Mars, as well as subsurface seismic volumes. However, an alternative source of topographic relief exists along US Gulf of Mexico and SE Atlantic coastal plains, which are regions generally considered flat. Alluvial ridges, built from aggraded

river-channel deposits, act as drainage divides between topographically lower regions where net-erosional tributary drainage networks develop. These tributary networks route fluid and solids from the bounding ridges to the coastline. The erosional relief produced by these networks provides additional space for later riverine deposits to accumulate, thus influencing how coastal river-channel belts are preserved in the stratigraphic record. To demonstrate the connection between this erosional topography and preserved overlying channel belts, both features were mapped in a 3D seismic volume offshore of the Brazos River delta, Texas, USA. Well-preserved fluvial channel belts are consistently mapped on top of surfaces possessing shorter, disorganized channelized features. These surfaces represent the erosional tributary surfaces of coastal tributary basins. The belts sitting above these surfaces record the occupation and filling of these basins by larger river systems. The erosional relief of a basin plus the constructional relief of the bordering ridges provides enough vertical space to prevent deposit reworking, which results in well-preserved belts recording 'strangely ordinary' transport conditions, and importantly, create a preservation mechanism that is both widespread and independent of allogenic forcings such as sea-level change and subsidence.

INTRODUCTION

External forcings, such as subsidence and sea-level change, are classically considered the primary controls on channel-belt preservation[1–6]. Fluvial channel belts are, however, commonly preserved over km to 10s of km in locations where such continuity is not expected due to low subsidence rates[7,8] that do not quickly remove these deposits from the active layer of surface erosion that would dissect older channel belts. At the dune scale, the larger bar-form topography can drive relatively rapid dune sedimentation and can provide topographic protection from later erosional reworking, leading to well-preserved deposits recording ordinary transport conditions[9,10,11]. Is there a source of larger-scale topography capable of preserving fluvial channel-belts in a similar way? Incised valleys fill this role[11–13], but well-preserved channel belts are not limited to valley fills[8,14]. Drainage basins across the coastal plains of the US Gulf of Mexico and southeastern Atlantic states[15,16] could provide up to 10s of m of relief for the potential preservation of channel-belt segments 10s of km in length[16] (Fig. 1). Raised alluvial ridges, constructed by active coastal rivers, act as effective drainage divides between basins that develop smaller-scale erosional tributary channel networks to drain water and sediment to the coastline (Fig. 1). This drainage limits floodplain aggradation while creating additional erosional relief[16] (Fig. 1).

We hypothesize that when larger-scale, primarily depositional rivers are re-routed into adjacent tributary basins by channel avulsion, they deposit channel-belt strata below topographic levels associated with the reworking depths of subsequent river thalwegs. This would preserve a 'strangely ordinary'[14] channel belt within an autogenic source of topography, much as a dune is preserved in front of a river bar[9]. Since 3D seismic volumes are exceedingly useful in imaging the preservation of ancient fluvial systems[8,11,12,17–25], the proposed hypothesis is tested herein using a 3D seismic volume to map fluvial channel belts preserved in the subsurface Gulf of Mexico offshore of the Brazos River, TX, USA (Fig. 2).. We sought to identify the stratigraphic context of well-preserved fluvial channel belts, hypothesizing that a distinct stratigraphic representation of the basal surfaces of coastal tributary basins exists that preserved channel belts overlie. In this study, the term "channel belt" is defined as the sum total of all channel-filling deposits left by a river, regardless of how much, or how little, lateral migration and aggradation is recorded[26–29].

TYPES OF CHANNELIZED DEPOSITS AND THEIR STRATIGRAPHIC CONTEXT

Two populations of channelized features were identified in each of the four survey zones (Fig. 2). The division between these populations is visually apparent (Fig. 3) and supported quantitatively by a statistical rejection of similar lengths and widths (Table 1; Fig. 4A). Of the 156 mapped channelized features, 17 define a population of longer features, and the remaining 139 define a population of shorter features (Table 1). To test the model that the shorter channelized features define the erosional basal

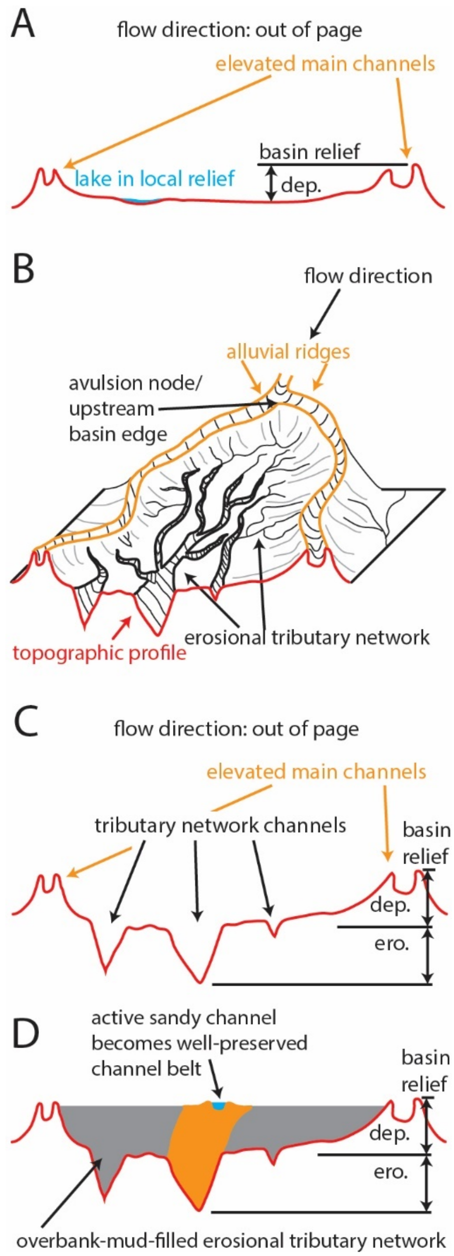

Figure 1 – A: Schematic transect between two raised alluvial ridges without the development of an erosional tributary network[16]*. Relief only forms from the decrease in sedimentation away from the main channels. While some local relief can create lakes, the overall relief is less than in panels B and C. B: Three-dimensional illustration of an erosional tributary network developed within a basin confined and bounded by alluvial ridges*[16]*. Alluvial ridges built by larger, sand-transporting channels (orange) define the basin boundaries. The erosional tributary network is drawn using black lines. The topographic profile at the edge*

of the diagram is shown with the red line, with the erosional channels generating v-shaped incisions. C: The red line showing relief in panels A and B. This relief is generated due to decreased sedimentation away from the channel (A), as well as the erosional tributary network channels (B). D: A sandy depositional channel has avulsed into the basin, where it has filled the basin with a sandy channel belt and muddy overbank deposits.

Table 1 – Geometry of the short and long channelized features. A two-sample Kalmogorov Smirnov test rejects the lengths ($p \ll 0.001$) and widths ($p = 0.001$) from each population as from the same distribution.

	Short (n = 139)	**long (n = 17)**
length		
mean (m) ± standard error (m)	368 ± 16	5,251 ± 729
minimum (m)	95	1,644
maximum (m)	1,043	13,074
standard deviation (m) ± standard error (m)	188 ± 11	3,005 ± 531
feature-averaged width		
mean (m) ± standard error (m)	155 ± 4	250 ± 39
minimum (m)	72	140
maximum (m)	276	831
standard deviation (m) ± standard error (m)	48 ± 3	159 ± 28

surface of a tributary drainage basin that was later filled by more continuous channel belts, the stratigraphic positions of the longer channelized features were compared to an interpolated 3D surface fitted to all the shorter features in each zone, and extending across the entirety of the zone. The fitted surface thus represents the erosional basal surface of a basin.

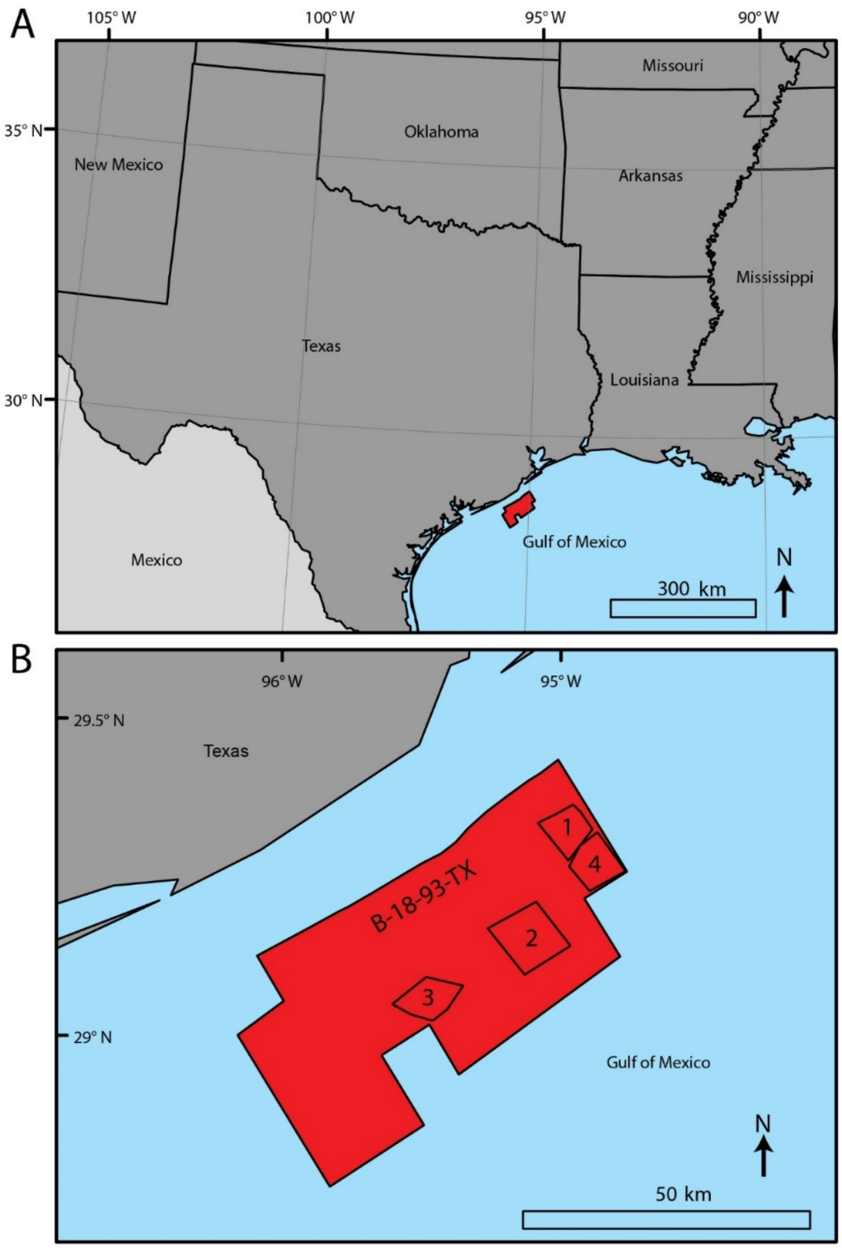

Figure 2 – A: Location map for the offshore seismic survey B-18-93-TX. The spatial extent of the survey is mapped in red. B: Zoom in to the survey area, with the mapped extent of the four studied zones presented in Figure 3.

Using horizontal slices at different depths (Fig. 3), histograms of depth in units of milliseconds of two-way-travel time (ms TWT) (Fig. 4), and depth profiles (Fig. 5), comparisons of the stratigraphic positions of the hypothesized basal surfaces against the longer channelized features in each zone were conducted. It was found that a consistent stratigraphic arrangement of the long channelized features and the hypothesized basal surfaces in zones 1-3 exists, where shorter channelized features occur ~ 0 to 60 ms TWT beneath the longer channelized features (Figs. 4). There is no instance in the dataset of a group of longer channelized features that are positioned directly beneath a surface defined by shorter features, which would be inconsistent with the proposed hypothesis.

Both types of channelized features occur in zone 4 in a similar arrangement, but exist within a larger topographic container not observed in zones 1-3 (Figs. 3 and 4). Instead, the zone 4 basal surface is a larger-scale topographic container, which has a distinct distribution of depth values, including a range 3 times larger than the other zones (~120 ms TWT vs. 40-50 ms TWT; Fig. 4) and a long tail towards shallower depths (Fig. 4E). In zone 4 variance horizontal slices, this surface has a scalloped shape and marks the western boundary of the channel-belt cluster (Fig. 3).

AUTOGENIC AND ALLOGENIC PRESERVATION

The zone 4 package of channel belts is interpreted as the filling of an incised valley based on: i) scalloped wall geometry (Fig. 3E-F), which is formed by outer-bank erosion during river migration[7,30,31], and ii) the total thickness of the fill (Fig. 4E). The preservation of channel belts over several km within this valley is consistent with the demonstrated significance of hierarchical topography when setting up the preservation of fluvial channel belts[23], but in this case represents an allogenic source of erosional relief: most likely sea-level change. Shorter channelized features in the valley fill form intersecting patterns in the time slices, and are interpreted as erosional rills or 1st-order channels, which are observed in other seismic volumes[11,32].

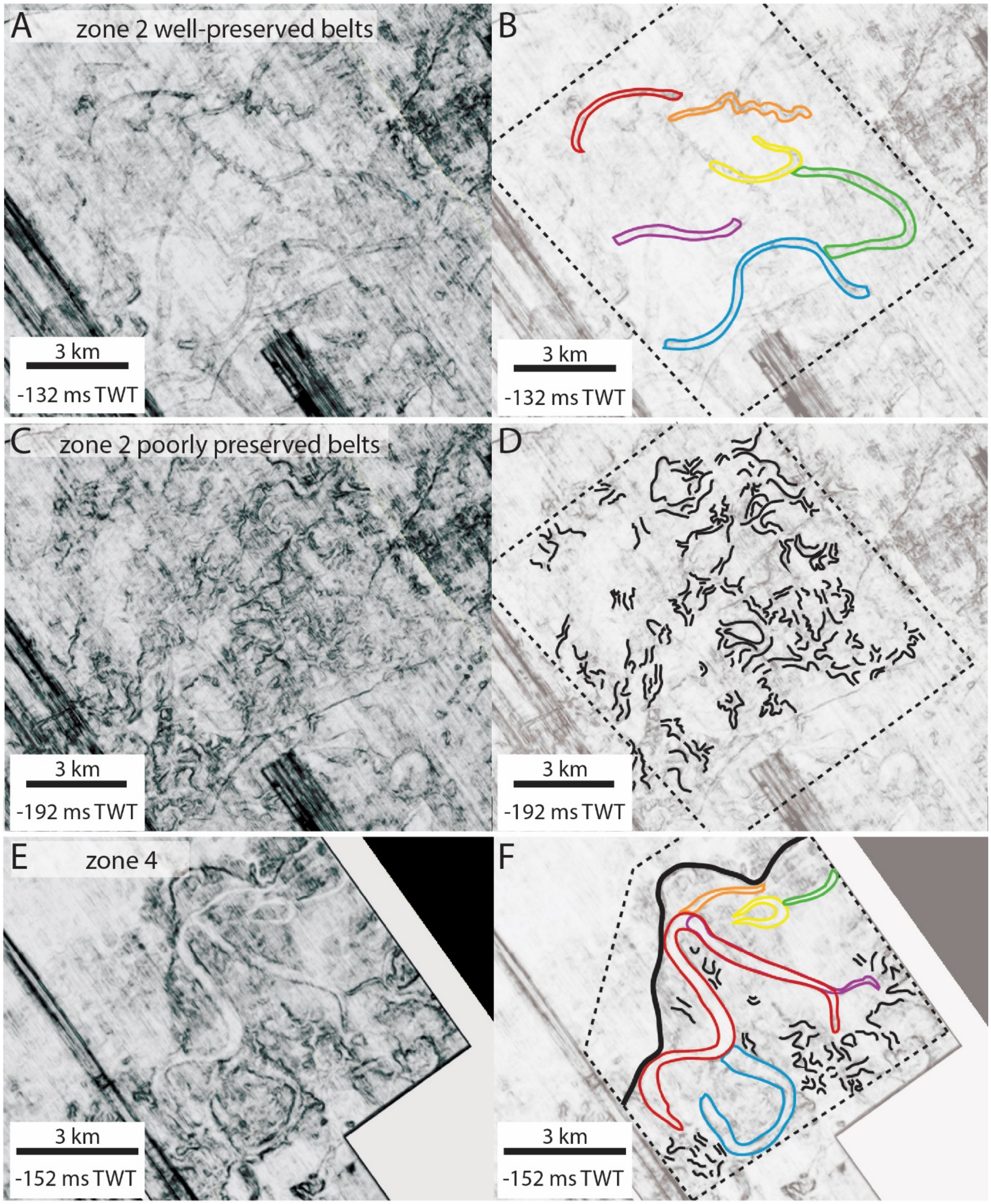

Figure 3 – Horizontal slices from the variance volume showing long channelized features (colored lines), short channelized features (black lines), and the region over which basal surfaces were fit to the short

channelized features (dashed polygons). Increasingly negative values (ms TWT) represent increasing depth below the sea floor, with 0 ms TWT at sea level. The location of each zone is shown in Figure 2. A: Time slice of zone 2 at -132 ms TWT. B: Interpretation of panel A showing 6 long channelized features. C: Time slice of zone 2 at -192 ms TWT. D: Interpretation of panel C, showing many short channelized features. These are interpreted to define the basal surfaces of coastal basins housing the well-preserved channel belts above. E: Time slice of zone 4 at -152 ms TWT. F: Interpretation of panel K, showing 6 distinct long channelized features and several short channelized features. The scalloped surface bounding the channelized features is mapped in a bold, solid black line. The channel belts in this zone are filling an incised valley with a border following the scalloped surface.

Conversely, the findings of zones 1-3 demonstrate that an incised valley is not the only possible source of channel-belt preserving relief. The channel belts in these zones are mappable over comparable distances, because similar to the zone 4 belts within a valley, they have not been post-depositionally reworked, and they maintain an impedance contrast with the surrounding sediment, which is likely due to a persistent contact between sandy channel fill and adjacent muds. Also, the shorter features (Fig. 3) are interpreted as the same erosional rills and channels later filled by muds as observed in the valley.

The stratigraphic arrangement of the hypothesized basal surface and the channel belts is shown in the zone 2 depth profiles presented in Figure 5, and highlights the fact that basal surfaces consistently underlie well-preserved channel belts. The stratigraphic arrangement of these two sedimentologically contrasting deposits (an erosional surface bounding preserved channel belts) thus supports the hypothesized filling of erosional tributary drainages by avulsive, sandy rivers and associated overbank muds, particularly where the channel belts exist within the range of elevations occupied by the basal surface (Fig. 4). Those which exist 10s of ms above those surfaces may be housed within the constructional

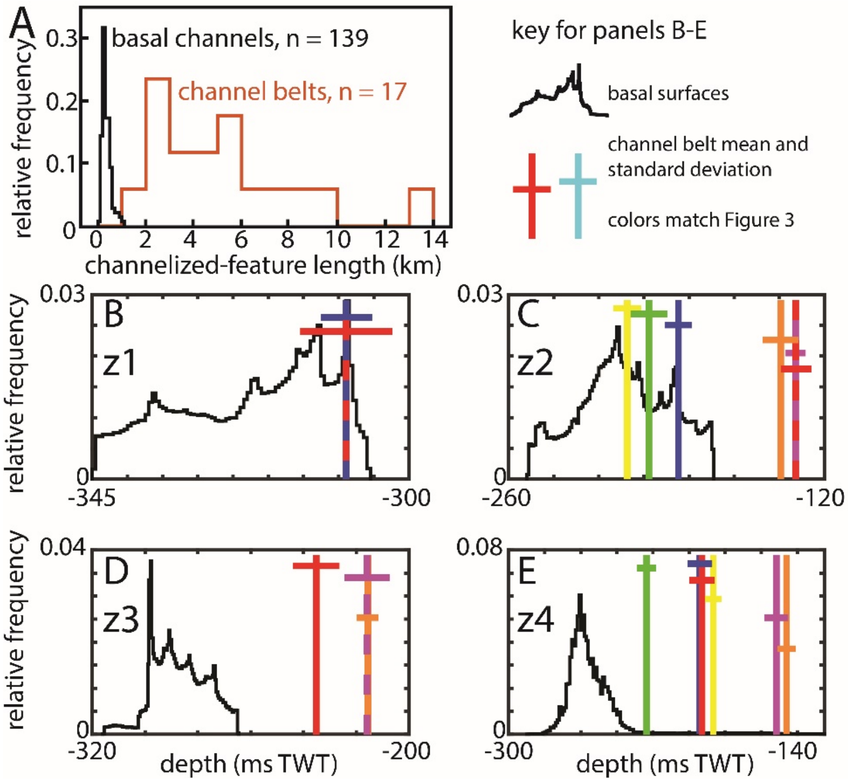

Figure 4 – A: Histogram comparing the two distinct channel belt populations based on their length normalized to their mean width. B-D: Black line histograms showing the distribution of depths for basal surfaces in each zone. Depth is measured in milliseconds of two-way-travel time, which has a value of zero at sea level, with larger negative values representing greater depths into the subsurface. Colored vertical lines are placed at the mean depths of each well-preserved channel belt, with the standard deviation around the mean represented by the cross. Belts not within the depth range of basal surfaces may occupy stratigraphically higher but acoustically transparent surfaces (zone 2's red, orange, and magenta belts; all belts in zone 3). Line colors match belt colors in Fig. 4. E: Same as panels B-D, but the basal surface of zone 4 is an incised valley (Fig. 4F), with the floor represented by the mode of the distribution, and the valley wall represented by the long, shallowing tail of the distribution heading towards -140 ms TWT.

155

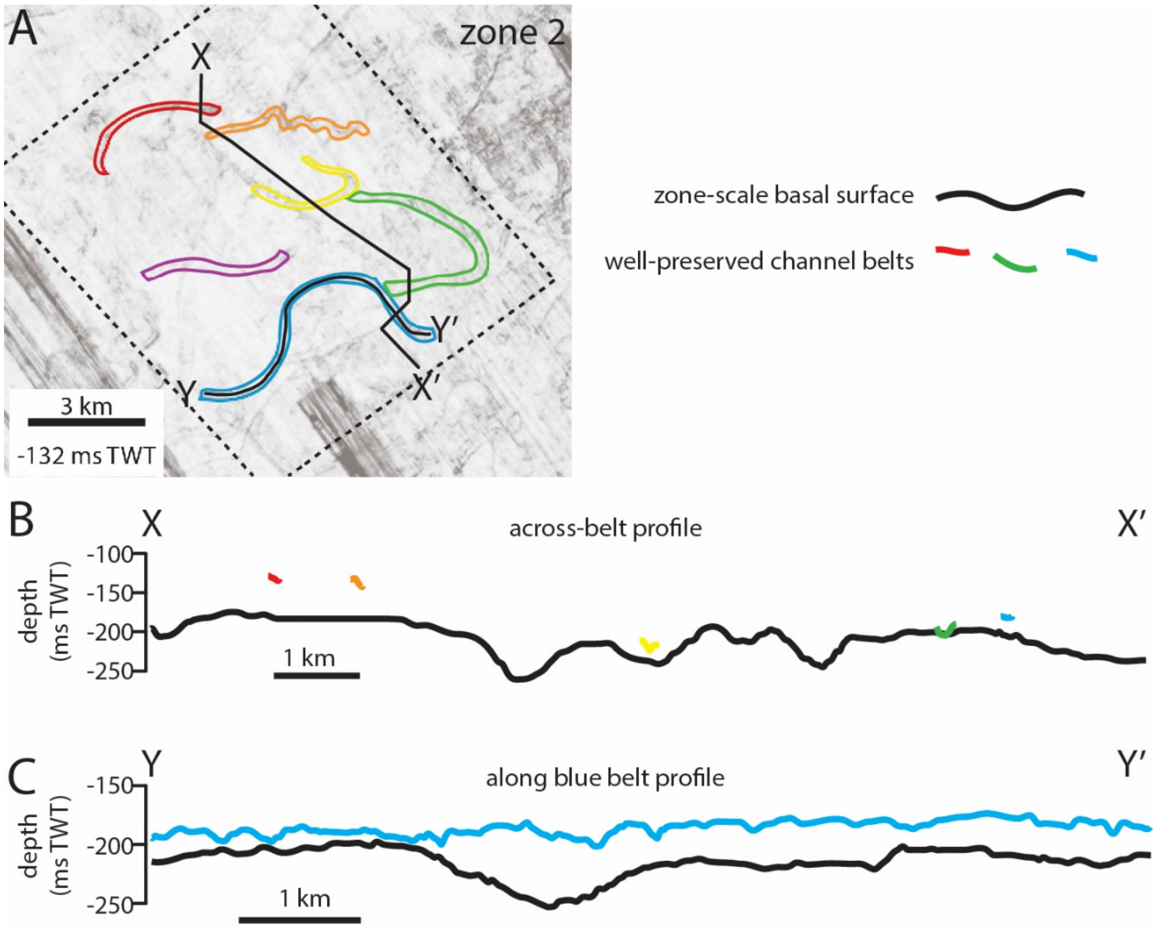

156 *Figure 5 – A: Variance time slice of zone 2 at -132 ms TWT showing the 6 long channelized features. Two*
157 *cross-sections are labeled. X-X' runs roughly perpendicular to the channelized features, intersecting five*
158 *of the six. Y-Y' runs along the blue channelized feature. B: Depth profiles along transect X-X' of the zone-*
159 *scale basal surface (black line) and long channelized features (color lines, same colors as panel A). Belts*
160 *sit less than 60 ms TWT above the basal surface. Lateral distance is marked with a scale bar. C: Depth*
161 *profile along transect Y-Y', which follows the blue channelized feature. The blue channelized feature is*
162 *consistently within 10 to a few 10s of ms TWT above the basal surface.*

163

range of relief associated with these basin (Fig. 1), or within stratigraphically higher but acoustically transparent basins. The latter interpretation may actually represent most of these basins, as the basins floors are mostly defined along mud-mud contacts.

These coastal tributary basins therefore represent an autogenic source of relief to preserve channel belts. In modern systems, these basins are more numerous and widespread than sources of allogenic relief such as incised valleys[16], and are potentially responsible for a large fraction of preserved channel belts in the stratigraphic record. Therefore, this newly documented means of channel-belt preservation must be considered when deciphering allogenic forcings, and likely extends to the preserved channel belts exposed at the surface of Mars near interpreted paleolakes and oceans[31,33,34].

Lastly, this autogenic preservation mechanism functions independent of basin subsidence. For instance, there exists a discrepancy between channel-belt preservation and subsidence rates in the Mississippi River delta[14]. Belts from 4 to 30 km in length are preserved, but the time required to create accommodation through subsidence is 10-50 times greater than avulsion frequency. This can be explained by deposition that occurs rapidly and locally over short timescales, which also transitions laterally over longer timescales[35]. The coastal basin preservation mechanism proposed in this study is a way to drive this rapid fluvial sedimentation and preservation, while simultaneously creating relief that will drive later episodes of rapid sedimentation at adjacent locations.

CONCLUSIONS

The development and filling of coastal tributary basins throughout the modern US Gulf of Mexico coast preserves fluvial channel belts in the stratigraphic record of the Gulf of Mexico without the requirement of an incised valley and, importantly, in the absence of high enough subsidence rates to create channel-belt-scale accommodation on avulsion timescales[14]. Furthermore, the formation of these basins may also be an important control on channel-belt clustering[36]. We posit that, because such preservation has been observed in other parts of the world beyond the extent of incised valleys[11,22], these basins commonly aid the preservation of channel belts across Earth by acting as a higher hierarchical source of topography, leading to the preservation of non-catastrophic deposits, i.e. the 'strange ordinariness', observed in the fluvial stratigraphic record[14]. A considerable fraction of preserved channel belts exhumed on Earth[29,37–40] and the surface of Mars[33,34,41–50] were therefore likely deposited within these basins. However, further investigations are needed to test the consistency of the findings of this study , which include coasts both similar and dissimilar to the Gulf of Mexico in terms of dominant processes, and other alluvial systems where these tributary basins may develop between channels, such as foreland-basin megafans/distributive fluvial systems[39,51,52]. Additionally, the lengths of channel belts can be further developed as a constraint on channel kinematics and filling of ancient channels, especially in seismic volumes or remote sensing datasets where belt thickness, an important recorded of channel kinematics[27–29], cannot be well constrained.

ACKNOWLEDGEMENTS

We thank Zoltan Sylvester and Joel Johnson for helpful early reviews of this manuscript, and Mike Lamb for helpful discussions. We thank the United States Geologic Survey for maintaining the National Archive of Marine Seismic Surveys at http://walrus.wr.usgs.gov/namss/. BTC acknowledges funding from The University of Texas at Austin Graduate School, the Jackson School of Geosciences, and the RioMAR Industry Consortium.

METHODS

A 3D seismic reflection volume of the Brazos River delta was downloaded from the National Archive of Marine Seismic Surveys (NAMSS; volume B-18-93-TX). This data volume was collected in 1993 and covered an area of ~2,300 km^2 from 15 km to 50 km offshore Texas (Fig. 2), with lines spaced 20 m apart and a 4 ms sampling rate. The median frequency of the volume is 38 Hz. Assuming similar subsurface acoustic velocities as other parts of the Mississippi River delta subsurface (1,900 m/s – 2,700 m/s)[7,8,23], wavelengths ranged from ~50-70 m. A reasonable estimate of vertical resolution is 1/4 the wavelength, or 13-18 m in this case[7,8,21,23]. This study was purposely restricted to the first 1000 milliseconds of acoustic wave two-way-travel time (ms TWT) because it had the highest frequency content for the reflected acoustic waves and afforded the best possible resolution of imaged strata. Stratigraphic surfaces were mapped in cross section using the Petrel software. This mapping was done is an amplitude volume because it provided the greatest vertical resolution. Channelized features were also imaged in map view using horizontal slices from a variance volume that highlighted discontinuity in the acoustic properties of deposits and therefore accentuated the edges of channelized features[7,53,54]. Note that a small degree of vertical integration goes into the production of a variance volume, and that the observations of a horizontal slice average data from above and below the plane[53]. Horizontal slices from the variance volume were used to map channel belts and the disorganized channelized features defining surfaces with erosionally generated relief. The basal surfaces of channelized features were mapped across the feature's lateral extent as observed in the time slice variance image, using truncated reflectors as a guide. Surfaces mapped in the along-belt direction were then used to tie cross sections to less obvious views. Next, surfaces interpolated between mapped horizons were converted to grids of points with XYZ coordinates, where a distribution of Z values (depth in units of ms TWT) was extracted from each surface to help quantify its stratigraphic position. The basal surfaces are clipped by 5% at either end in Figure 4.

After cross-sectional mapping, selected variance horizontal slices were exported from Petrel and into ArcGIS, in order to perform more robust planview mapping operations[13]. The centerline length and average width of channel belts were calculated by first mapping the opposite long edges of each feature as a series of ~2 m spaced points with XY coordinates. A local measurement of width was made from each point along one edge to the nearest point on the opposite edge using an automated script, and a centerline point was placed halfway between the two points. Width measurements were averaged for each feature, and the centerline length was calculated as the sum of the distances between successive centerline points.

REFERENCES

1. Leeder, M. R. A Quantitative Stratigraphic Model for Alluvium, with Special Reference to Channel Deposit Density and Interconnectedness. 587–596 (1977).
2. Bridge, J. S. & Leeder, M. R. A simulation model of alluvial stratigraphy. *Sedimentology* **26**, 617–644 (1979).
3. Wright, P. V. & Marriott, S. B. The sequence stratigraphy of fluvial depositional systems: the role of floodplain sediment storage. *Sedimentary Geology* **86**, 203–210 (1993).
4. Allen, J. R. L. Studies in fluviatile sedimentation: an exploratory quantitative model for the architecture of avulsion-controlled alluvial suites. *Sedimentary Geology* **21**, 129–147 (1978).
5. Hajek, E. A. & Heller, P. L. Flow-Depth Scaling In Alluvial Architecture and Nonmarine Sequence Stratigraphy: Example from the Castlegate Sandstone, Central Utah, U.S.A. *Journal of Sedimentary Research* **82**, 121–130 (2012).
6. Chamberlin, E. P. & Hajek, E. A. Using bar preservation to constrain reworking in channel-dominated fluvial stratigraphy. *Geology* **47**, 531–534 (2019).
7. Armstrong, C. P. 3D seismic geomorphology and stratigraphy of the late Miocene to Pliocene Mississippi River Delta : fluvial systems and dynamics. (2012).
8. Armstrong, C., Mohrig, D., Hess, T., George, T. & Straub, K. M. Influence of growth faults on coastal fluvial systems: Examples from the late Miocene to Recent Mississippi River Delta. *Sedimentary Geology* **301**, 120–132 (2014).
9. Reesink, A. J. H. *et al.* Extremes in dune preservation: Controls on the completeness of fluvial deposits. *Earth-Science Reviews* **150**, 652–665 (2015).

10. Miall, A. D. Updating uniformitarianism: stratigraphy as just a set of ‘frozen accidents’. *Geological Society, London, Special Publications* **404**, 11–36 (2015).

11. Miall, A. D. Architecture and Sequence Stratigraphy of Pleistocene Fluvial Systems in the Malay Basin, Based on Seismic Time-Slice Analysis. *AAPG Bulletin* **86**, 1201–1216 (2002).

12. Alqahtani, F. A., Johnson, H. D., Jackson, C. A.-L. & Som, M. R. B. Nature, origin and evolution of a Late Pleistocene incised valley-fill, Sunda Shelf, Southeast Asia. *Sedimentology* **62**, 1198–1232 (2015).

13. Alqahtani, F. A., Jackson, C. A.-L., Johnson, H. D. & Som, M. R. B. Controls On the Geometry And Evolution of Humid-Tropical Fluvial Systems: Insights From 3D Seismic Geomorphological Analysis of the Malay Basin, Sunda Shelf, Southeast AsiaF.A. ALQAHTANI ET AL.3D SEISMIC GEOMORPHOLOGY. *Journal of Sedimentary Research* **87**, 17–40 (2017).

14. Paola, C., Ganti, V., Mohrig, D., Runkel, A. C. & Straub, K. M. Time Not Our Time: Physical Controls on the Preservation and Measurement of Geologic Time. *Annual Review of Earth and Planetary Sciences* **46**, 409–438 (2018).

15. Willett, S. D., McCoy, S. W., Perron, J. T., Goren, L. & Chen, C.-Y. Dynamic Reorganization of River Basins. *Science* **343**, 1248765–1248765 (2014).

16. Swartz, J. M., Cardenas, B. T., Mohrig, D. & Passalacqua, P. From Distributary to Tributary: Formation of Channel Networks Set by Depositional Processes. (in review).

17. Wood, L. J. Quantitative Seismic Geomorphology of Pliocene and Miocene Fluvial Systems in the Northern Gulf of Mexico, U.S.A. *Journal of Sedimentary Research* **77**, 713–730 (2007).

18. Hubbard, S. M. *et al.* Seismic geomorphology and sedimentology of a tidally influenced river deposit, Lower Cretaceous Athabasca oil sands, Alberta, Canada. *Bulletin* **95**, 1123–1145 (2011).

19. Jobe, Z. R., Howes, N. C. & Auchter, N. C. Comparing submarine and fluvial channel kinematics: Implications for stratigraphic architecture. *Geology* **44**, 931–934 (2016).

20. Fernandes, A. M., Törnqvist, T. E., Straub, K. M. & Mohrig, D. Connecting the backwater hydraulics of coastal rivers to fluvio-deltaic sedimentology and stratigraphy. *Geology* **44**, 979–982 (2016).

21. Zeng, H. What is seismic sedimentology? A tutorial. *Interpretation* **6**, SD1–SD12 (2018).

22. Martin, J. *et al.* The Stratigraphically Preserved Signature of Persistent Backwater Dynamics in a Large Paleodelta System: The Mungaroo Formation, North West Shelf, Australia. *Journal of Sedimentary Research* **88**, 850–872 (2018).

23. Straub, K. M., Paola, C., Mohrig, D., Wolinsky, M. A. & George, T. Compensational Stacking of Channelized Sedimentary Deposits. *Journal of Sedimentary Research* **79**, 673–688 (2009).

24. *Landscapes on the Edge: New Horizons for Research on Earth's Surface*. 12700 (National Academies Press, 2010). doi:10.17226/12700.

25. Durkin, P. R., Hubbard, S. M., Holbrook, J. & Boyd, R. Evolution of fluvial meander-belt deposits and implications for the completeness of the stratigraphic record. *GSA Bulletin* **130**, 721–739 (2018).

26. Blum, M. D. & Törnqvist, T. E. Fluvial responses to climate and sea-level change: a review and look forward. *Sedimentology* **47**, 2–48 (2000).

27. Gibling, M. R. Width and Thickness of Fluvial Channel Bodies and Valley Fills in the Geological Record: A Literature Compilation and Classification. *Journal of Sedimentary Research* **76**, 731–770 (2006).

28. Jerolmack, D. J. & Mohrig, D. Conditions for branching in depositional rivers. *Geology* **35**, 463–466 (2007).

29. Cardenas, B. T. *et al. Anatomy of exhumed river-channel belts: Bedform- to belt-scale kinematics of the Cretaceous Cedar Mountain Formation, Utah, USA*. https://osf.io/zw4hr (2019) doi:10.31223/osf.io/zw4hr.

30. Zaitlin, B. A., Dalrymple, R. W. & Boyd, R. The Stratigraphic Organization of Incised-Valley Systems Associated with Relative Sea-Level Change. (1994).

31. Cardenas, B. T., Mohrig, D. & Goudge, T. A. Fluvial stratigraphy of valley fills at Aeolis Dorsa, Mars: Evidence for base-level fluctuations controlled by a downstream water body. *GSA Bulletin* **130**, 484–498 (2018).

32. Reijenstein, H. M., Posamentier, H. W. & Bhattacharya, J. P. Seismic geomorphology and high-resolution seismic stratigraphy of inner-shelf fluvial, estuarine, deltaic, and marine sequences, Gulf of ThailandSeismic Geomorphology and Stratigraphy in the Gulf of Thailand. *AAPG Bulletin* **95**, 1959–1990 (2011).

33. Goudge, T. A., Mohrig, D., Cardenas, B. T., Hughes, C. M. & Fassett, C. I. Stratigraphy and paleohydrology of delta channel deposits, Jezero crater, Mars. *Icarus* **301**, 58–75 (2018).

34. DiBiase, R. A., Limaye, A. B., Scheingross, J. S., Fischer, W. W. & Lamb, M. P. Deltaic deposits at Aeolis Dorsa: Sedimentary evidence for a standing body of water on the northern plains of Mars. *Journal of Geophysical Research: Planets* **118**, 1285–1302 (2013).

35. Sadler, P. M. & Jerolmack, D. J. Scaling laws for aggradation, denudation and progradation rates: the case for time-scale invariance at sediment sources and sinks. *Geological Society, London, Special Publications* **404**, 69–88 (2015).

36. Hajek, E. A., Heller, P. L. & Sheets, B. A. Significance of channel-belt clustering in alluvial basins. *Geology* **38**, 535–538 (2010).

37. Mohrig, D., Heller, P. L., Paola, C. & Lyons, W. J. Interpreting avulsion process from ancient alluvial sequences: Guadalope-Matarranya system (northern Spain) and Wasatch Formation (western Colorado). *GSA Bulletin* **112**, 1787–1803 (2000).

38. Cuevas Martínez, J. L. *et al.* Exhumed channel sandstone networks within fluvial fan deposits from the Oligo-Miocene Caspe Formation, South-east Ebro Basin (North-east Spain). *Sedimentology* **57**, 162–189 (2010).

39. Owen, A., Nichols, G. J., Hartley, A. J., Weissmann, G. S. & Scuderi, L. A. Quantification of a Distributive Fluvial System: The Salt Wash DFS of the Morrison Formation, SW U.S.A.QUANTIFICATION OF THE SALT WASH DFS. *Journal of Sedimentary Research* **85**, 544–561 (2015).

40. Hayden, A. T. *et al.* Formation of sinuous ridges by inversion of river-channel belts in Utah, USA, with implications for Mars. *Icarus* **332**, 92–110 (2019).

41. Burr, D. M. *et al.* Pervasive aqueous paleoflow features in the Aeolis/Zephyria Plana region, Mars. *Icarus* **200**, 52–76 (2009).

42. Kite, E. S. *et al.* Stratigraphy of Aeolis Dorsa, Mars: Stratigraphic context of the great river deposits. *Icarus* **253**, 223–242 (2015).

43. Davis, J. M., Balme, M., Grindrod, P. M., Williams, R. M. E. & Gupta, S. Extensive Noachian fluvial systems in Arabia Terra: Implications for early Martian climate. *Geology* **44**, 847–850 (2016).

44. Davis, J. M. *et al.* A Diverse Array of Fluvial Depositional Systems in Arabia Terra: Evidence for mid-Noachian to Early Hesperian Rivers on Mars. *Journal of Geophysical Research: Planets* **124**, 1913–1934 (2019).

45. Hughes, C. M., Cardenas, B. T., Goudge, T. A. & Mohrig, D. Deltaic deposits indicative of a paleo-coastline at Aeolis Dorsa, Mars. *Icarus* **317**, 442–453 (2019).

46. Williams, R. M. E., Irwin, R. P., Burr, D. M., Harrison, T. & McClelland, P. Variability in martian sinuous ridge form: Case study of Aeolis Serpens in the Aeolis Dorsa, Mars, and insight from the Mirackina paleoriver, South Australia. *Icarus* **225**, 308–324 (2013).

47. Jacobsen, R. E. & Burr, D. M. Dichotomies in the fluvial and alluvial fan deposits of the Aeolis Dorsa, Mars: Implications for weathered sediment and paleoclimate. *Geosphere* **13**, 2154–2168 (2017).

48. Lefort, A., Burr, D. M., Nimmo, F. & Jacobsen, R. E. Channel slope reversal near the Martian dichotomy boundary: Testing tectonic hypotheses. *Geomorphology* **240**, 121–136 (2015).

49. Matsubara, Y. *et al.* River meandering on Earth and Mars: A comparative study of Aeolis Dorsa meanders, Mars and possible terrestrial analogs of the Usuktuk River, AK, and the Quinn River, NV. *Geomorphology* **240**, 102–120 (2015).

50. Fassett, C. I. & Head, J. W. Fluvial sedimentary deposits on Mars: Ancient deltas in a crater lake in the Nili Fossae region. *Geophysical Research Letters* **32**, (2005).

51. Horton, B. K. & DeCelles, P. G. Modern and ancient fluvial megafans in the foreland basin system of the central Andes, southern Bolivia: implications for drainage network evolution in fold-thrust belts. *Basin Research* **13**, 43–63 (2001).

52. Weissmann, G. S. *et al.* Prograding Distributive Fluvial Systems—Geomorphic Models and Ancient Examples. in *New Frontiers in Paleopedology and Terrestrial Paleoclimatology: Paleosols and Soil Surface Analog Systems* (ed. Driese, S. G.) 131–147 (SEPM (Society for Sedimentary Geology), 2013). doi:10.2110/sepmsp.104.16.

53. Bahorich, M. & Farmer, S. 3-D seismic discontinuity for faults and stratigraphic features: The coherence cube. *The Leading Edge* **14**, 1053–1058 (1995).

54. Liu, J. & Marfurt, K. J. Instantaneous spectral attributes to detect channels. *GEOPHYSICS* **72**, P23–P31 (2007).